CHEMISTRY
AN ASIAN JOURNAL

DOI: 10.1002/asia.200800236

A DFT Study on the Reaction Pathways for Carbon−Carbon Bond-Forming Reactions between Propargylic Alcohols and Alkenes or Ketones Catalyzed by Thiolate-Bridged Diruthenium Complexes

Ken Sakata,*[a] Yoshihiro Miyake,[b] and Yoshiaki Nishibayashi[b]

Abstract: The reaction pathways of two types of the carbon−carbon bond-forming reactions catalyzed by thiolate-bridged diruthenium complexes have been investigated by density-functional-theory calculations. It is clarified that both carbon−carbon bond-forming reactions proceed through a ruthenium–allenylidene complex as a common reactive intermediate. The attack of π electrons on propene or the vinyl alcohol on the ruthenium–allenylidene complex is the first step of the reaction pathways. The reaction pathways are different after the attack of nucleophiles on the ruthenium–alkynyl complex. In the reaction with propene, the carbon−carbon bond-forming reaction proceeds through a stepwise process, whereas in the reaction with vinyl alcohol, it proceeds through a concerted process. The interactions between the ruthenium–allenylidene complex and propene or vinyl alcohol have been investigated by applying a simple way of looking at orbital interactions.

Keywords: alcohols • alkenes • density functional calculations • ketones • ruthenium

Introduction

Recently, chalcogenolate-bridged diruthenium complexes[1] such as $[Cp^*RuCl(\mu_2\text{-}YR)]_2$ ($Cp^* = \eta^5\text{-}C_5Me_5$, Y = S, Se, Te) have been found to promote propargylic substitution reactions of propargylic alcohols with not only various heteroatom-centered but also carbon-centered nucleophiles to afford the corresponding propargylic-substituted products in high yields with a complete selectivity.[2] This catalytic reaction has an advantage over the well-known Nicholas reaction, which needs several steps and a stoichiometric amount of $[Co_2(CO)_8]$ for the preparation of propargylic-substituted products.[3] Some experimental results on the isolation and investigation of allenylidene[4,5] complexes indicate that this catalytic propargylic substitution reaction proceeds through the ruthenium–allenylidene complexes as key intermediates.[6] More recently, Nakamura and co-workers have calculated the reaction pathway of the propargylic substitution reaction with alcohol as a nucleophile by using the density functional theory (DFT) method and found the synergistic effect of two ruthenium atoms in the diruthenium complexes.[7]

As a related work, the carbon−carbon bond-forming reactions between propargylic alcohols and alkenes have been reported to give the corresponding 1,5-enynes in good yields with a complete selectivity (Scheme 1).[8] This catalytic reaction is considered to proceed by means of allenylidene–ene reactions in which the C_β−C_γ double bond of the allenylidene complex may function as an enophile, however, the detailed reaction pathway has not yet been clarified.

More recently, we have investigated the reactions between propargylic alcohols and 1,3-conjugated dienes to give the corresponding dienyne compounds in good to high yields.[9] Some results of experimental and theoretical studies indicate that this catalytic reaction proceeds through a stepwise reaction pathway.[9] In this catalytic reaction, the alkynyl complex bearing a cationic γ-carbon, which is a resonance structure of the allenylidene complex, is found to work as a key intermediate. This result prompted us to reconsider the reaction pathway of the allenylidene–ene reactions shown in Scheme 1. We have now envisaged the DFT calculation at the B3LYP/631LAN level of this catalytic reaction by using

---

[a] Dr. K. Sakata
Faculty of Pharmaceutical Sciences
Hoshi University
Ebara, Shinagawa-ku, Tokyo, 142-8501 (Japan)
Fax: (+81) 3-5498-5078
E-mail: sakata@hoshi.ac.jp

[b] Dr. Y. Miyake, Prof. Dr. Y. Nishibayashi
Institute of Engineering Innovation
The University of Tokyo
Yayoi, Bunkyo-ku, Tokyo 113-8656 (Japan)

Supporting information for this article is available on the WWW under http://dx.doi.org/10.1002/asia.200800236.

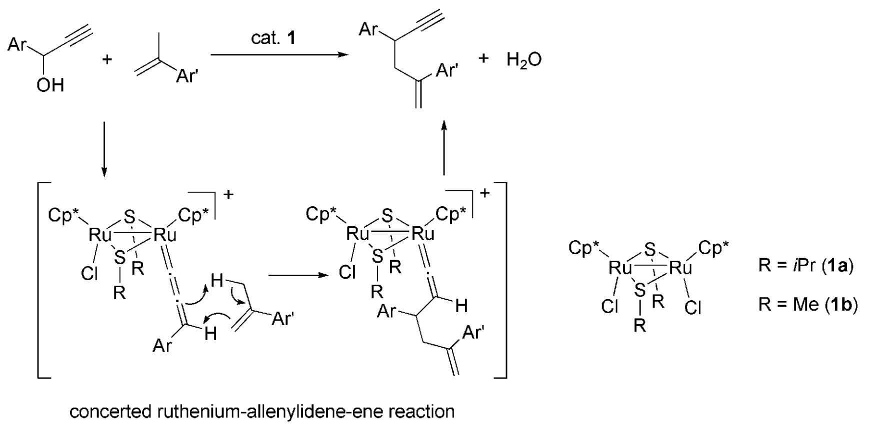

Scheme 1. Carbon-carbon bond-forming reactions between propargylic alcohols and alkenes.

a model reaction between $[CpRuCl(\mu_2\text{-SMe})_2RuCp(=C=C=CH_2)]^+$ (**1**; Cp = η^5-C_5H_5) and propene (Scheme 2).

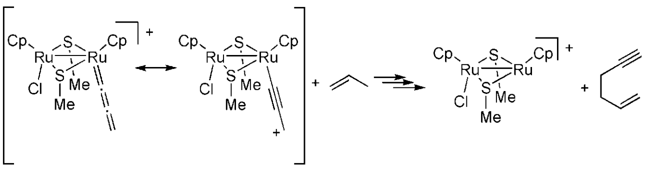

Scheme 2. Model reaction between **1** and propene.

Results and Discussion

The starting allenylidene complex **1** was previously proposed by Nakamura and co-workers (Scheme 3).[7] This previous study has shown that the present level of theory (B3LYP/631LAN level) gives reliable results for the reaction of the allenylidene complex.[7] Optimized structures and relative-energy diagrams for the model reaction of **1** with propene are shown in Figures 1 and 2, respectively. At first, the complexation of the allenylidene complex **1** with the C=C bond in propene gave the initial composite system **2a**. As shown in Figures 1 and 2, the distances between the C_γ atom and the C_1 atom and between the C_γ atom and the C_2 atom at **2a** are 3.073 and 3.221 Å, respectively, and the complexation energy is only 2.9 kcal mol^{-1}. Next, the nucleophilic attack of π electrons of propene on the C_γ atom in the allenylidene complex took place through **TS2a–3a** to give the intermediate complex **3a** in which the weak C_γ–C_1 bond is formed (the bond distance is 1.708 Å and the Mayer bond order is 0.742). As shown in Figure 2, the energies of **TS2a–3a** and **3a** relative to the initial state (**1**+propene), Δ*E*, are +2.7 and +2.0 kcal mol^{-1}, respectively, which are considerably small. Subsequently, the hydrogen atom on the C_3 atom was easily transferred into the C_β atom through **TS3a–4a** to give the stable vinylidene complex **4a**. The Δ*E* of **TS3a–4a** and **4a** are +3.0 and −26.3 kcal mol^{-1}, respectively. The Gibbs free energies of **TS2a–3a**, **3a**, **TS3a–4a**, and **4a** relative to the initial state (**1**+propene) at 298.15 K, Δ*G*, are +16.8, +16.7, +16.5, and −11.4 kcal mol^{-1}, respectively. In a real system, only α-methylstyrene derivatives are available for this catalytic carbon–carbon bond-forming reaction.[8a] When a phenyl group is introduced at the C_2 position of propene, the resonance stabilization,[8a] which makes the relative energy lower, is predicted in not only **3a** but also **TS2a–3a** and **TS3a–4a**. These results indicate that the reaction of propene addition to the allenylidene complex **1** should proceed through a stepwise process in which the weak C_γ–C_1 bond formation is followed by the transfer of the hydrogen atom into the C_β atom. A similar stepwise mechanism has already been proposed for the carbonyl–ene reaction catalyzed by bis(oxazoline) copper(II) complexes.[10]

The nucleophilic attack of π electrons of propene on the electrophilic C_γ atom of the allenylidene ligand through **TS2a–3a** is easily recognized by regarding it as the reaction

Abstract in Japanese:

硫黄架橋二核ルテニウム錯体を用いたプロパルギルアルコールとアルケン及びケトンとの炭素-炭素結合生成反応について、モデル反応系を用いた密度汎関数法計算により反応経路の検討を行った。プロペン及びビニルアルコールとのいずれの反応系においても、求核剤内に存在するπ電子のルテニウム—アルキニル錯体への求核攻撃が反応の初期段階であるが、その後の反応経路は求核剤の種類により異なることを明らかにした。

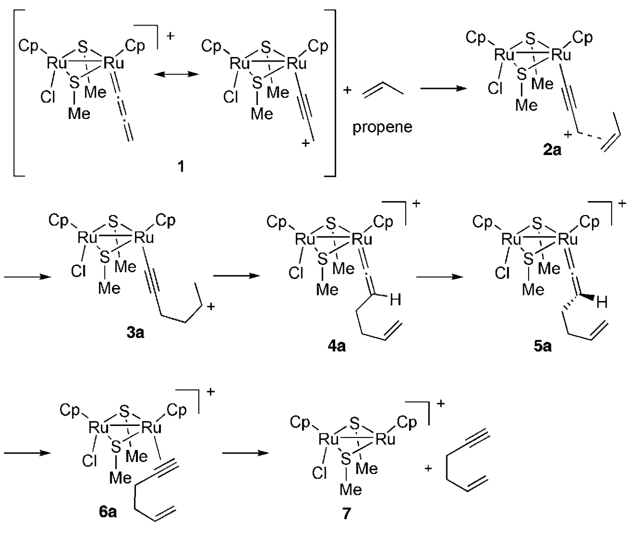

Scheme 3. Reaction pathways of the reaction between **1** and propene.

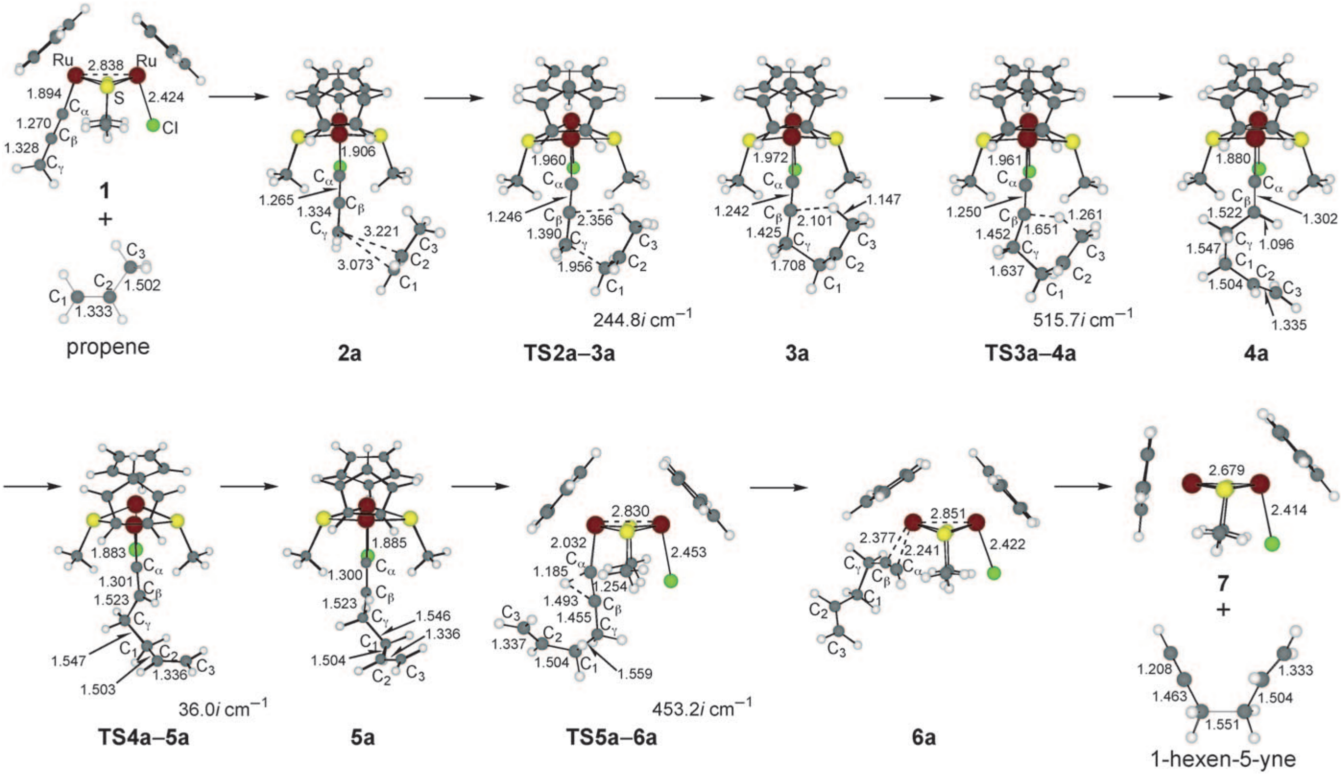

Figure 1. Optimized structures of stationary points for the reaction of $[CpRuCl(\mu_2\text{-}SMe)_2RuCp(=C=C=CH_2)]^+$ with propene. Bond lengths are in Å.

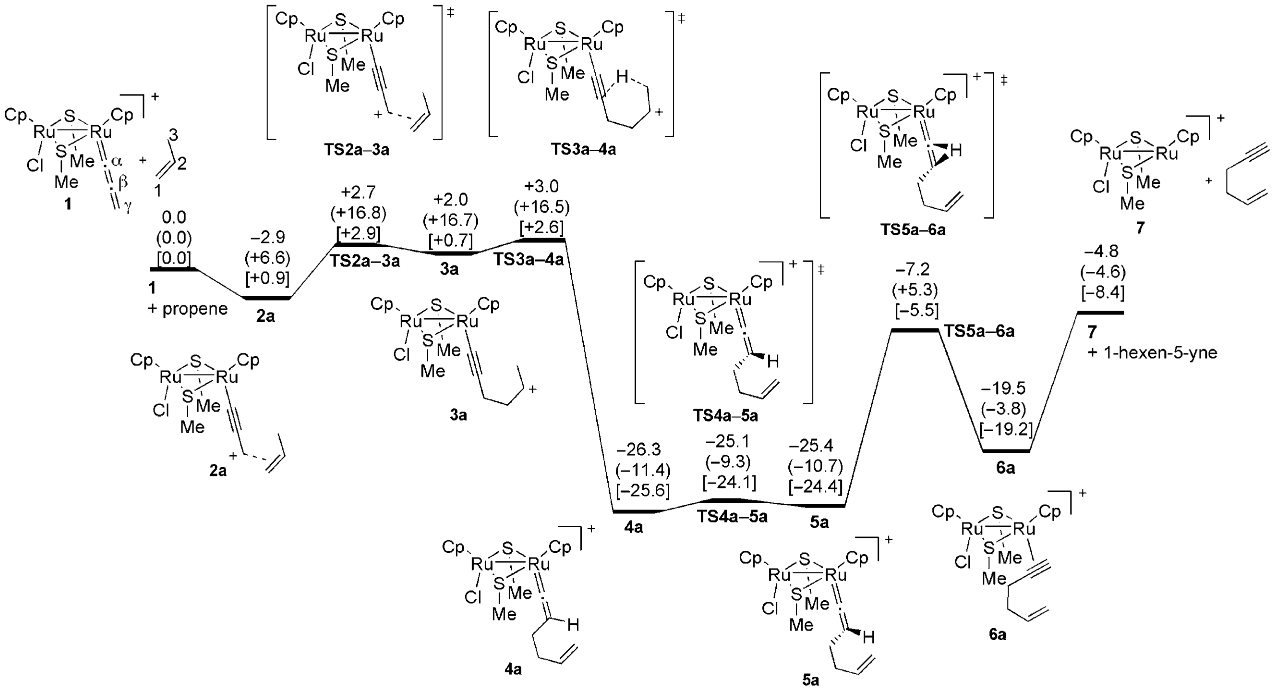

Figure 2. Relative energy diagram (kcal mol^{-1}) for the model reaction of $[CpRuCl(\mu_2\text{-}SMe)_2RuCp(=C=C=CH_2)]^+$ with propene. Values in parentheses are relative Gibbs free energies at 298.15 K in the gas phase. Values in square brackets are relative energies in solution.

between the ruthenium–alkynyl resonance structure in the allenylidene complex and the π bond in propene as shown in Scheme 3. The calculated charge at the terminal CH_2 group in **1** was found to be +0.038 in the Mulliken population analysis (MPA) and +0.274 in the natural population analysis (NPA). For orbital interactions in the reaction of the mono-ruthenium allenylidene complex, Bruce indicated that the nucleophilic attack is expected at C_α and C_γ atoms based on the extended Hückel molecular orbitals.[11] We analyzed electron delocalization in the nucleophilic attack at **TS2a–3a** in terms of orbital interaction by utilizing the interaction frontier orbital (IFO) scheme.[12] The bond-order matrix $\boldsymbol{P}$ was defined in terms of the canonical Kohn–Sham orbitals of the two fragments, that is, propene and the ruthenium–allenylidene complex. Then, the occupied orbitals ϕ of propene and the unoccupied orbitals ψ of the ruthenium–allenylidene complex were transformed simultaneously within each fragment in such a way that only a few sets of paired orbitals of the two fragments give significant values for the off-diagonal intermolecular part of $\boldsymbol{P}$. The analysis showed that electron delocalization from propene to the ruthenium–allenylidene complex at **TS2a–3a** is described practically by a pair of orbitals (ϕ_1'; ψ_1'), as is illustrated in Figure 3a. The orbital ϕ_1' is the π-bonding orbital localized on the C_1–C_2 bond while the orbital ψ_1' has a large amplitude on the C_γ atom of the allenylidene complex. This pair of orbitals is responsible for the bond formation between the C_γ atom and the C_1 atom. This result shows that the π-occupied orbital in propene plays an important role in the nucleophilic attack of propene into the C_γ atom of the ruthenium–allenylidene complex. π Electrons in propene corresponded to the lone-pair electrons of the heteroatom in the case of the reaction of the ruthenium–allenylidene complex with heteroatom-centered nucleophiles. Thus, both reactions of the ruthenium–allenylidene complexes with propene and heteroatom-centered nucleophiles belong to the same type of reactions. Moreover, the orbital phases of the Ru–C_α and C_β–C_γ bonds in the ψ_1' orbital are out of phase and so the electron delocalization represented by the pair (ϕ_1'; ψ_1') was expected to make these bonds loosen. As shown in Figure 1, these bond distances certainly become longer as the reaction proceeds (1.894 Å (**1**)→1.906 Å (**2a**)→1.960 Å (**TS2a–3a**)→ 1.972 Å (**3a**) in the Ru–C_α bond and 1.328 Å (**1**)→1.334 Å (**2a**)→1.390 Å (**TS2a–3a**)→1.425 Å (**3a**) in the C_β–C_γ bond). On the other hand, the orbital phase of the C_α–C_β bond is in phase, so the bond distance becomes shorter (1.270 Å (**1**)→1.265 Å (**2a**)→1.246 Å (**TS2a–3a**)→1.242 Å (**3a**)). This corresponds to the increase of the weight of the ruthenium–alkynyl resonance structure in the ruthenium–allenylidene complex.

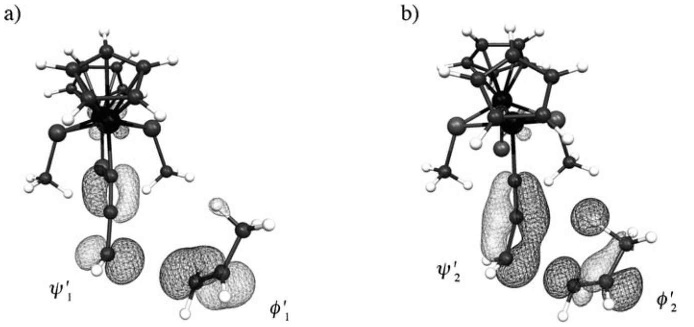

Figure 3. Pairs of interacting orbitals. a) (ϕ_1'; ψ_1') of **TS2a–3a** and b) (ϕ_2'; ψ_2') of **TS3a–4a**, calculated at the B3LYP/631LAN level of theory. The positive and negative regions of orbitals are discriminated by the shade of black. Note that the two fragments possess the same structures as those at the transition state, but their positions are chosen separated so as not to mix the two orbitals up.

The vinylidene complex **4a** was converted into another vinylidene complex **5a** in which the direction of the vinylidene moiety is vertical to that in **4a** (Figure 1 and 2). The ΔE of **5a** is $-25.4\,\mathrm{kcal\,mol^{-1}}$, which is higher than **4a** by $0.9\,\mathrm{kcal\,mol^{-1}}$. The α,β-hydrogen migration in **5a** proceeded through **TS5a–6a** to give the π complex **6a**. As proposed in the previous paper,[7] no C–H σ complex is located for the diruthenium catalytic system, indicating that the transition state for the α,β-hydrogen migration connects a vinylidene complex to a π complex. The ΔE of **TS5a–6a** is $-7.2\,\mathrm{kcal\,mol^{-1}}$, which is much lower than those of **TS2a–3a** and **TS3a–4a** ($+2.7$ and $+3.0\,\mathrm{kcal\,mol^{-1}}$). In the final step of the reaction, the energy change for the dissociation of **6a** into the coordinatively unsaturated complex (**7**) and 1-hexen-5-yne is $14.7\,\mathrm{kcal\,mol^{-1}}$. From the viewpoint of the free energy, the ΔG of **5a**, **TS5a–6a**, **6a**, and the final state (**7**+1-hexen-5-yne) are -10.7, $+5.3$, -3.8, and $-4.6\,\mathrm{kcal\,mol^{-1}}$, respectively, and the free-energy difference between **6a** and (**7**+1-hexen-5-yne) is only $0.8\,\mathrm{kcal\,mol^{-1}}$. These results indicate that the dissociation of **6a** easily occurred to afford **7** and 1-hexen-5-yne. Nakamura and co-workers examined the reaction pathways of the reactions of di- and mono-ruthenium complexes with propargylic alcohol by using DFT calculations and pointed out that the catalyst turnover step, which corresponds to the dissociative exchange of the product with the substrate, readily takes place in the case of the diruthenium system because of the compensation of the coordinative unsaturation by the stronger Ru–Ru interaction.[7] Our present result is consistent with their results. For the whole reaction pathway, the isomerization of **5a** into **6a** is considered to be a rate-determining step. In fact, we observed a substantial isotope effect ($k_H/k_D=4$) when the reaction was carried out with [D_3]α-methylstyrene-methyl in place of α-methylstyrene.[8a] The k_H/k_D was calculated to be 2.3 at 60 °C in the present study. We also estimated the effect of dichloroethane as a solvent by the single-point PCM calculations. The relative energies in solution are shown in Figure 2. The results show that the solvent effect is small.

Results from the DFT calculations for the allenylidene–ene reactions prompted us to investigate the reaction pathway of propargylic substitution reactions of propargylic alcohols with ketones, such as acetone as carbon-centered nucleophiles. As described in previous papers,[13] we considered that the propargylic alkylation with acetone proceeds through the nucleophilic attack of the enol form of acetone on the C_γ atom of the allenylidene complex, although the detailed reaction pathway remains unknown (Scheme 4). As a model reaction between **1** and enol, we replaced a methyl group of propene with a hydroxy group in which an isoelectronic vinyl alcohol of propene was regarded as the smallest model molecule of the enol. Herein, we describe the DFT

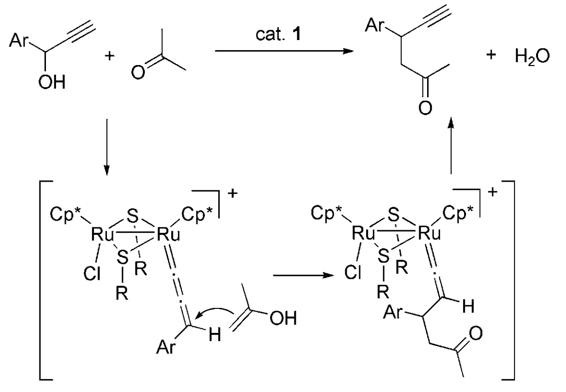

Scheme 4. Propargylic substitution reactions of propargylic alcohols with acetone.

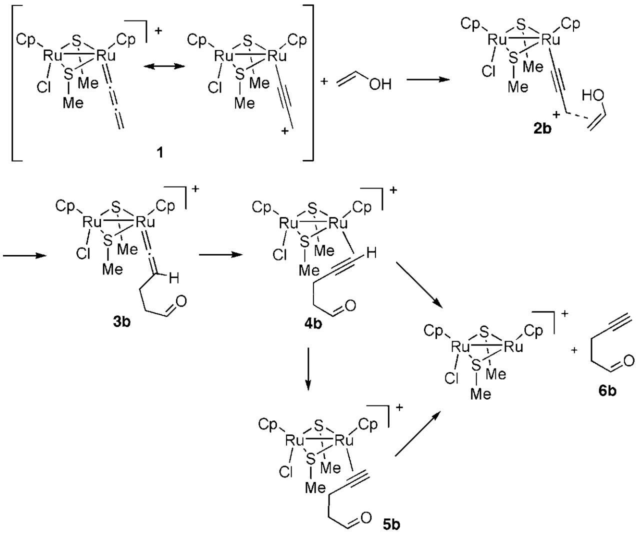

Scheme 5. Reaction pathways of the reaction between **1** and vinyl alcohol.

calculation of the propargylic alkylation by using this model reaction.

The starting allenylidene complex **1** was previously proposed by Nakamura and co-workers (Scheme 5).[7] Optimized structures and a relative-energy diagram for the model reaction of **1** with vinyl alcohol are shown in Figures 4 and 5, respectively. The initial composite system **2b**, which corresponds to **2a** in the reaction of **1** with propene, is formed between **1** and the vinyl alcohol. The complexation energy of **2b** is 5.6 kcal mol^{-1} and the distances between the C_γ atom and the C_2 atom and between the C_γ atom and the C_1 atom in **2b** are 2.973 Å and 3.127 Å, respectively, which are slightly shorter than those in **2a**. In the subsequent transition state **TS2b–3b**, the C_γ–C_2 distance is 2.265 Å, which is longer than that in **TS2a–3a** (1.956 Å). The energy of **TS2b–3b** relative to the initial state (**1**+vinyl alcohol), ΔE, is −4.7 kcal mol^{-1} and the energy difference between **2b** and **TS2b–3b** is only 0.9 kcal mol^{-1}. In this case, the π-occupied orbital in the vinyl alcohol also attacks the electrophilic C_γ atom in the ruthenium–allenylidene complex, although the vinyl alcohol includes the lone-pair electrons in the oxygen atom, which is another nucleophilic site.

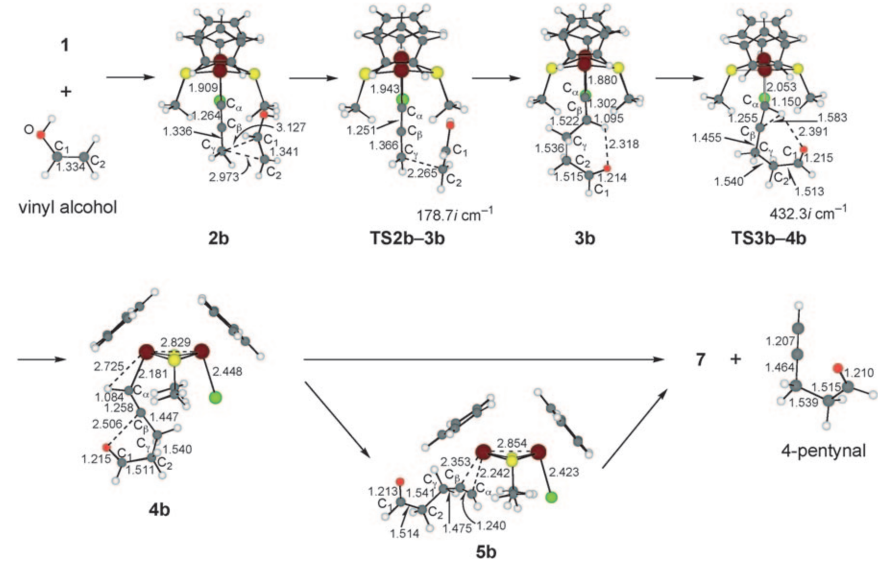

Figure 4. Optimized structures of stationary points for the reaction of [CpRuCl(μ_2-SMe)$_2$RuCp(=C=C=CH$_2$)]$^+$ with vinyl alcohol. Bond lengths are in Å.

The stationary structure of the intermediate complex that corresponds to **3a** could not be located in the model reaction of **1** with vinyl alcohol. Results of the intrinsic reaction coordinate (IRC) calculation[14] starting from **TS2b–3b** are shown in Figure 6. Figure 6 shows that the reaction pathway is not a purely synchronous concerted process. That is, the C_γ–C_2 bond is formed and then the O–H bond dissociates rapidly to give the vinylidene complex (**3b**). The ΔE of **3b** is −41.7 kcal mol^{-1}, which indicates that the vinylidene complex **3b** is considerably stable. In sharp contrast with the formation of the vinylidene complex **4a** via **3a** as an intermediate from the reaction of **1** with propene, the direct formation of **3b** was observed from the reaction of **1** with vinyl alcohol. In the reaction of **1** with vinyl alcohol, the formation of **3b** is concerted, but the mechanism involves two asynchronous steps. This type of reaction, which is concerted but not synchronous, is called the two-stage reaction by Dewar.[15]

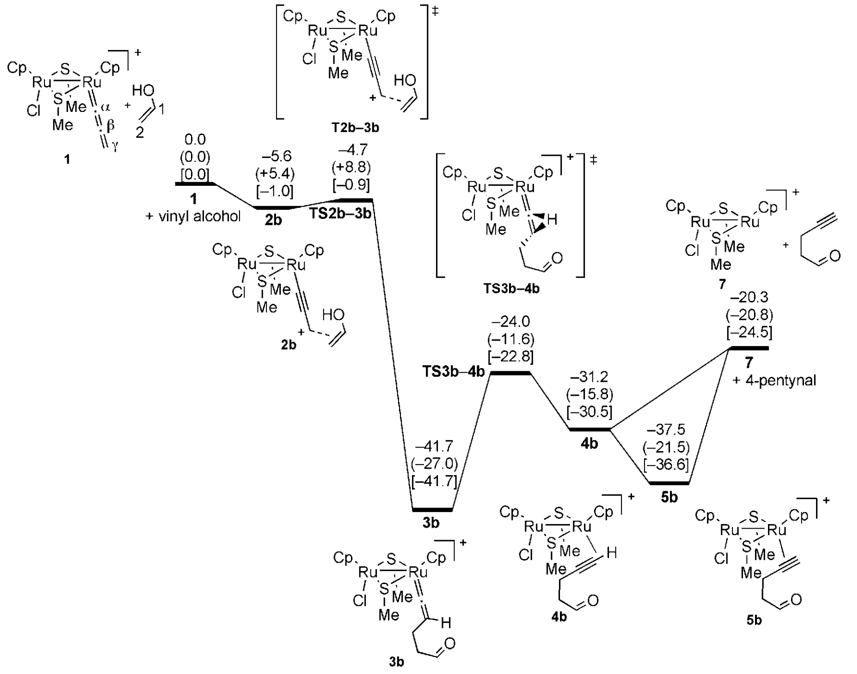

Figure 5. Relative-energy diagram (kcal mol^{-1}) for the model reaction of [CpRuCl(μ_2-SMe)$_2$RuCp(=C=C=CH$_2$)]$^+$ with vinyl alcohol. Values in parentheses are relative Gibbs free energies at 298.15 K in the gas phase. Values in square brackets are relative energies in solution.

The α,β-hydrogen transfer in **3b** proceeds through **TS3b–4b** to afford a σ complex (**4b**; Figure 4 and 5). In the σ complex **4b**, the C_α atom of the terminal alkyne is coordinated with the Ru atom, and the C_β atom weakly interacts with the oxygen atom. The ΔE of **TS3b–4b** and **4b** are −24.0 and −31.2 kcal mol^{-1}, respectively. Then, the σ complex **4b** is transformed into the π complex (**5b**), which is more stable than **4b** by 6.3 kcal mol^{-1} in energy. The ΔE of the final state (**7**+4-pentynal) is −20.3 kcal mol^{-1}, which is higher than those of **4b** and **5b** (−31.2 and −37.5 kcal mol^{-1}). From the viewpoint of the free energy, the differences between **4b** and (**7**+4-pentynal) and between **5b** and (**7**+4-pentynal) are 5.0 and 0.7 kcal mol^{-1}, respectively, which are small. These results indicate that the dissociation of both complexes **4b** and **5b** easily occurs to afford **7** and 4-pentynal in the same way as the reaction of **1** with propene. Thus, the reaction of **1** with vinyl alcohol also proceeds smoothly through ruthenium–alkynyl complexes as key intermediates.

Finally, a difference between the two reaction pathways is discussed. Results from calculations for the reaction of **1** with propene showed that this carbon−carbon bond-forming reaction proceeds through a stepwise reaction process, whereas those for the reaction with vinyl alcohol indicated that it proceeds through a concerted reaction process. These two reaction pathways have the same asynchronous mechanism in which the nucleophilic attack of the carbon atom of propene or vinyl alcohol on the C_γ atom (first step) is followed by the transfer of the hydrogen atom (second step). However, there is no intermediate complex along the reaction pathway of the reaction with vinyl alcohol while the intermediate complex (**3a**) exists in the reaction with propene. The existence of the intermediate complex **3a** provides important clues to understand the reaction between propargylic alcohol and the 1,3-conjugated diene,[9] and of the intramolecular cyclization[16] by using the diruthenium complex as a catalyst. Energetically, the difference is caused by the large stability of the vinylidene complex **3b**. The ΔE of **3b** in the reaction system of the vinyl alcohol (−41.7 kcal mol^{-1}) is much lower than that of **4a** in the reaction system of propene

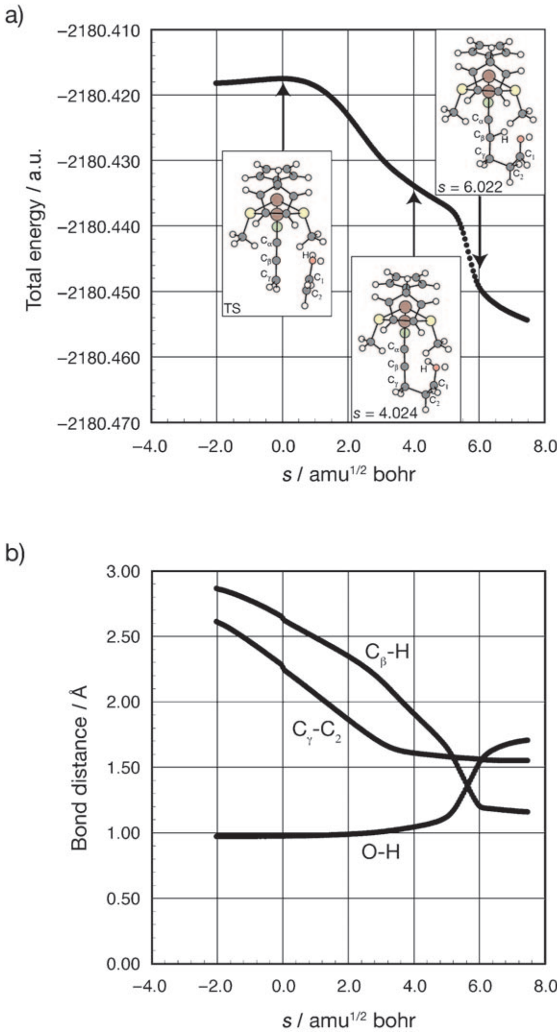

Figure 6. Potential energy curve (a) and geometrical changes (b) along the IRC starting from **TS2b–3b**.

($-26.3\,\text{kcal mol}^{-1}$). From the viewpoint of the electronic property, the NPA charges of the hydrogen atom that transfers into the C_β atom in **TS2a–3a**, **3a**, and **TS3a–4a** are +0.284, +0.307, and +0.314, respectively, in the case of the reaction system of propene. On the other hand, the NPA charges of the hydrogen atom in **TS2b–3b** and in the structure at the $s=4.024\,\text{amu}^{1/2}\cdot\text{bohr}$ along the IRC of **TS2b–3b** (see Figure 6a) are +0.512 and +0.533, respectively, which are more positive. The higher positive charge indicates the larger electron-acceptance ability of the hydrogen atom. In terms of orbital interactions between **1** and propene or vinyl alcohol, the electron delocalization from **1** to propene or vinyl alcohol comes to play an important role in the second step, which corresponds to the hydrogen transfer, whereas the opposite direction of the electron delocalization mostly dominates the first step corresponding to the nucleophilic attack on the C_γ atom. According to the IFO analysis[12], the electron delocalization from **1** to propene in **TS3a–4a** is described practically by a pair of interacting orbitals (ϕ_2'; ψ_2') illustrated in Figure 3b. The orbital ψ_2', which consists of occupied orbitals in the ruthenium–allenylidene part, is the π-bonding orbitals in the allenylidene ligand. The orbital ϕ_2', which consists of unoccupied orbitals in propene, has large amplitudes in the C_1–C_2 bond and in the hydrogen atom. The electron delocalization represented by the pair (ϕ_2'; ψ_2') is responsible for the bond forming between the C_β atom and the hydrogen atom and for the further strengthening of the C_γ–C_1 bond. In the case of the reaction system of vinyl alcohol, the electron delocalization from **1** to vinyl alcohol is expected to become larger as the reaction proceeds. In the structure along the IRC for **TS2b–3b** ($s=4.024\,\text{amu}^{1/2}\cdot\text{bohr}$), a pair of interacting orbitals that are similar in shape was also obtained.[17] The localization of the orbital ϕ_2' in the hydrogen atom (42.4%) is larger than that in **TS3a–4a** (27.0%), and the orbital ϕ_2' has the clear antibonding character in the O–H bond. These results indicate the difference in the acidity of the hydrogen atom after the nucleophilic attack on the C_γ atom. The acidity of the hydrogen atom in the O–H is higher than that in C–H (Scheme 6). This difference causes the facility of the hydrogen transfer into the C_β atom in the reaction of **1** with vinyl alcohol.

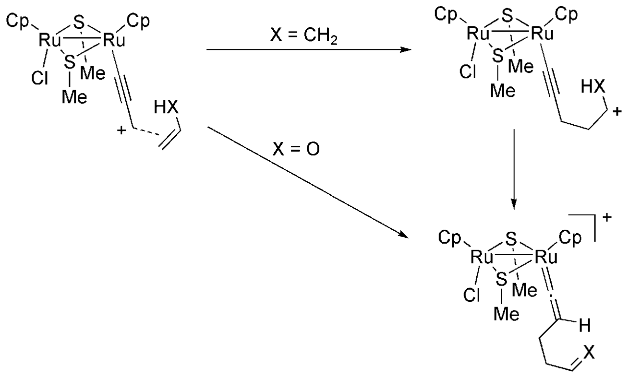

Scheme 6. Difference in the acidity of the hydrogen atom.

In summary, we have found the reaction pathways of two types of the carbon–carbon bond-forming reactions catalyzed by thiolate-bridged diruthenium complexes by DFT calculations. Both carbon–carbon bond-forming reactions proceed via ruthenium–allenylidene complexes as common reactive intermediates. The nucleophilic attack of propene or vinyl alcohol on a ruthenium–alkynyl complex, a resonance structure of ruthenium–allenylidene complex, is the first step of the reaction pathway. π Electrons in propene or vinyl alcohol play an important role in the first step. The reaction pathways are different after the attack of nucleophiles on the ruthenium–alkynyl complexes. That is, the carbon–carbon bond-forming reaction proceeds through a stepwise process in the reaction with propene, whereas it proceeds through a concerted process in the reaction with vinyl alcohol. This is caused by the difference in the acidity of the hydrogen atom that is transferred to the C_β atom. Both the present carbon–carbon bond-formation reactions and the reactions with the heteroatom-centered nucleophiles[7] are considered to be the same type of reactions. The findings described herein provide a chance to develop further novel catalytic activities of the ruthenium–allenylidene complexes including ruthenium–cumulenylidene complexes.[18]

Experimental Section

Computational Details

All DFT calculations were carried out with the Gaussian 03 program package.[19] Geometry optimization was performed by the Kohn–Sham DFT by using Becke's three-parameter hybrid method with the Lee, Yang, and Parr correlation functional (B3LYP).[20,21] Pople's 6–31G(d) basis set[22] for C, H, O, S, and Cl atoms and the LANL2DZ basis set[23] including a double-ζ valence basis set with the Hay–Wadt's effective core potential (ECP) for Ru atom were used for the Gaussian basis functions (denoted as 631 LAN). Theoretical harmonic vibrational frequencies were obtained at the same level of theory to verify each equibrium structure as a true energy minimum or a saddle point. The bond-order proposed by Mayer[24] and the atomic charges based on the MPA[25] and on the NPA[26] were obtained by means of the Kohn–Sham orbitals. For **2a**, **TS2a–3a**, **3a**, **TS3a–4a**, **2b**, and **TS2b–3b**, the stability analysis for solutions of the closed-shell Kohn–Sham equations[27] was performed to confirm that the obtained Kohn–Sham equations are stable. The solvent effects were estimated by performing the polarizable continuum model (PCM)[28] calculations with the integral equation formalism (IEF)[29] for the gas-phase optimized structures. Dichloroethane ($\varepsilon=10.36$) was used as the solvent and the united atom topological model applied on radii optimized at the PBE0/6–31G(d) level of theory (UAKS) was utilized for the IEF-PCM method.

Acknowledgements

This work was supported by Grants-in-Aid for Scientific Research for Scientific Research on Priority Areas (No. 18066003) and Young Scientists (S) (No. 19675002) from the Ministry of Education, Culture, Sports, Science and Technology, Japan. Some of the calculations were made at Research Center for Computational Science, Okazaki, Japan. KS is grateful to the Center for generous permission to use its computing facilities.

[1] Preparation of various chalcogenolate-bridged diruthenium complexes and their catalytic activity toward the propargylic substitution reactions, see: a) Y. Nishibayashi, H. Imajima, G. Onodera, M. Hidai, S. Uemura, *Organometallics* **2004**, *23*, 26; b) Y. Nishibayashi, H. Imajima, G. Onodera, Y. Inada, M. Hidai, S. Uemura, *Organometallics* **2004**, *23*, 5100.

[2] a) Y. Nishibayashi, I. Wakiji, M. Hidai, *J. Am. Chem. Soc.* **2000**, *122*, 11019; b) Y. Inada, Y. Nishibayashi, M. Hidai, S. Uemura, *J. Am. Chem. Soc.* **2002**, *124*, 15172; c) Y. Nishibayashi, M. D. Milton, Y. Inada, M. Yoshikawa, I. Wakiji, M. Hidai, S. Uemura, *Chem. Eur. J.* **2005**, *11*, 1433.

[3] a) K. M. Nicholas, *Acc. Chem. Res.* **1987**, *20*, 207 and references therein; b) A. J. M. Caffyn, K. M. Nicholas in *Comprehensive Organometallic Chemistry II, Vol. 12* (Eds.: E. W. Abel, G. A. Stone, G. Wilkinson), Pergamon, New York, **1995**, Chapter 7.1.

[4] For recent reviews, see: a) V. Cadierno, M. P. Gamasa, J. Gimeno, *Eur. J. Inorg. Chem.* **2001**, 571; b) C. Bruneau, P. H. Dixneuf, *Angew. Chem.* **2006**, *118*, 2232; *Angew. Chem. Int. Ed.* **2006**, *45*, 2176.

[5] a) B. M. Trost, J. A. Flygare, *J. Am. Chem. Soc.* **1992**, *114*, 5476; b) K.-L. Yeh, B. Liu, C.-Y. Lo, H.-L. Huang, R.-S. Liu, *J. Am. Chem. Soc.* **2002**, *124*, 6510; c) S. Datta, C.-L. Chang, K.-L. Yeh, R.-S. Liu, *J. Am. Chem. Soc.* **2003**, *125*, 9294; d) H.-C. Shen, H.-L. Su, Y.-C. Hsueh, R.-S. Liu, *Organometallics* **2004**, *23*, 4332.

[6] a) Y. Nishibayashi, Y. Inada, M. Hidai, S. Uemura, *J. Am. Chem. Soc.* **2002**, *124*, 7900; b) Y. Nishibayashi, M. Yoshikawa, Y. Inada, M. Hidai, S. Uemura, *J. Am. Chem. Soc.* **2002**, *124*, 11846; c) Y. Nishibayashi, M. Yoshikawa, Y. Inada, M. D. Milton, M. Hidai, S. Uemura, *Angew. Chem.* **2003**, *115*, 2785; *Angew. Chem. Int. Ed.* **2003**, *42*, 2681; d) Y. Nishibayashi, M. Yoshikawa, Y. Inada, M. Hidai, S. Uemura, *J. Org. Chem.* **2004**, *69*, 3408; e) M. D. Milton, G. Onodera, Y. Nishibayashi, S. Uemura, *Org. Lett.* **2004**, *6*, 3993; f) M. D. Milton, Y. Inada, Y. Nishibayashi, S. Uemura, *Chem. Commun.* **2004**, 2712; g) G. Onodera, H. Matsumoto, M. D. Milton, Y. Nishibayashi, S. Uemura, *Org. Lett.* **2005**, *7*, 4029; h) Y. Inada, Y. Nishibayashi, S. Uemura, *Angew. Chem.* **2005**, *117*, 7893; *Angew. Chem. Int. Ed.* **2005**, *44*, 7715; i) Y. Inada, M. Yoshikawa, M. D. Milton, Y. Nishibayashi, S. Uemura, *Eur. J. Org. Chem.* **2006**, 881; j) G. Onodera, Y. Nishibayashi, S. Uemura, *Organometallics* **2006**, *25*, 35; k) Y. Yamauchi, G. Onodera, K. Sakata, M. Yuki, Y. Miyake, S. Uemura, Y. Nishibayashi, *J. Am. Chem. Soc.* **2007**, *129*, 5175; l) H. Matsuzawa, Y. Miyake, Y. Nishibayashi, *Angew. Chem.* **2007**, *119*, 6608; *Angew. Chem. Int. Ed.* **2007**, *46*, 6488.

[7] S. C. Ammal, N. Yoshikai, Y. Inada, Y. Nishibayashi, E. Nakamura, *J. Am. Chem. Soc.* **2005**, *127*, 9428.

[8] a) Y. Nishibayashi, Y. Inada, M. Hidai, S. Uemura, *J. Am. Chem. Soc.* **2003**, *125*, 6060; b) Y. Nishibayashi, M. Yoshikawa, Y. Inada, M. Hidai, S. Uemura, *J. Am. Chem. Soc.* **2004**, *126*, 16066.

[9] M. Daini, M. Yoshikawa, Y. Inada, S. Uemura, K. Sakata, K. Kanao, Y. Miyake, Y. Nishibayashi, *Organometallics* **2008**, *27*, 2046.

[10] L. Morao, J. P. McNamara, I. H. Hillier, *J. Am. Chem. Soc.* **2003**, *125*, 628.

[11] M. I. Bruce, *Chem. Rev.* **1998**, *98*, 2797.

[12] a) K. Fukui, N. Koga, H. Fujimoto, *J. Am. Chem. Soc.* **1981**, *103*, 196; b) H. Fujimoto, N. Koga, I. Hataue, *J. Phys. Chem.* **1984**, *88*, 3539; c) H. Fujimoto, *Acc. Chem. Res.* **1987**, *20*, 448.

[13] a) Y. Nishibayashi, I. Wakiji, Y. Ishii, S. Uemura, M. Hidai, *J. Am. Chem. Soc.* **2001**, *123*, 3393; b) Y. Nishibayashi, G. Onodera, Y. Inada, M. Hidai, S. Uemura, *Organometallics* **2003**, *22*, 873; c) Y. Inada, Y. Nishibayashi, S. Uemura, *Angew. Chem.* **2005**, *117*, 7893; *Angew. Chem. Int. Ed.* **2005**, *44*, 7715.

[14] a) K. Fukui, *Acc. Chem. Res.* **1981**, *14*, 363; b) C. Gonzalez, H. B. Schlegel, *J. Chem. Phys.* **1989**, *90*, 2154.

[15] M. J. S. Dewar, *J. Am. Chem. Soc.* **1984**, *106*, 209.

[16] K. Fukamizu, Y. Miyake, Y. Nishibayashi, *J. Am. Chem. Soc.* **2008**, *130*, 10498.

[17] See the Supporting Information.

[18] Y. Yamauchi, M. Yuki, Y. Tanabe, Y. Miyake, Y. Inada, S. Uemura, Y. Nishibayashi, *J. Am. Chem. Soc.* **2008**, *130*, 2908.

[19] *Gaussian 03*, Revision D.02, M. J. Frisch, G. W. Trucks, H. B. Schlegel, G. E. Scuseria, M. A. Robb, J. R. Cheeseman, J. A. Montgomery, Jr., T. Vreven, K. N. Kudin, J. C. Burant, J. M. Millam, S. S. Iyengar, J. Tomasi, V. Barone, B. Mennucci, M. Cossi, G. Scalmani, N. Rega, G. A. Petersson, H. Nakatsuji, M. Hada, M. Ehara, K. Toyota, R. Fukuda, J. Hasegawa, M. Ishida, T. Nakajima, Y. Honda, O. Kitao, H. Nakai, M. Klene, X. Li, J. E. Knox, H. P. Hratchian, J. B. Cross, V. Bakken, C. Adamo, J. Jaramillo, R. Gomperts, R. E. Stratmann, O. Yazyev, A. J. Austin, R. Cammi, C. Pomelli, J. W. Ochterski, P. Y. Ayala, K. Morokuma, G. A. Voth, P. Salvador, J. J. Dannenberg, V. G. Zakrzewski, S. Dapprich, A. D. Daniels, M. C. Strain, O. Farkas, D. K. Malick, A. D. Rabuck, K. Raghavachari, J. B. Foresman, J. V. Ortiz, Q. Cui, A. G. Baboul, S. Clifford, J. Cioslowski, B. B. Stefanov, G. Liu, A. Liashenko, P. Piskorz, I. Komaromi, R. L. Martin, D. J. Fox, T. Keith, M. A. Al-Laham, C. Y. Peng, A. Nanayakkara, M. Challacombe, P. M. W. Gill, B. Johnson, W. Chen, M. W. Wong, C. Gonzalez, J. A. Pople, Gaussian, Inc., Wallingford, CT, **2004**.

[20] a) P. Hohenberg, W. Kohn, *Phys. Rev.* **1964**, *136*, B864; b) W. Kohn, L. J. Sham, *Phys. Rev.* **1965**, *140*, A1133.

[21] a) A. D. Becke, *J. Chem. Phys.* **1993**, *98*, 5648; b) C. Lee, W. Yang, R. G. Parr, *Phys. Rev. B* **1988**, *37*, 785; c) P. J. Stephens, F. J. Devlin, C. F. Chabalowski, M. J. Frich, *J. Phys. Chem.* **1994**, *98*, 11623.

[22] W. J. Hehre, L. Radom, P. v. R. Schleyer, J. A. Pople, *Ab Initio Molecular Orbital Theory*, Wiley, New York, **1986**.

[23] P. J. Hay, W. R. Wadt, *J. Chem. Phys.* **1985**, *82*, 284, 299.

[24] I. Mayer, *Chem. Phys. Lett.* **1983**, *97*, 270.

[25] R. S. Mulliken, *J. Chem. Phys.* **1955**, *23*, 1833, 1841, 2338, 2343.

[26] A. E. Reed, R. B. Weinstock, F. Weinhold, *J. Chem. Phys.* **1985**, *83*, 735.

[27] R. Bauernschmitt, R. Ahlrichs, *J. Chem. Phys.* **1996**, *104*, 9047.

[28] a) S. Miertus, E. Scrocco, J. Tomasi, *Chem. Phys.* **1981**, *55*, 117; b) J. Tomasi, M. Persico, *Chem. Rev.* **1994**, *94*, 2027.

[29] a) E. Cancès, B. Mennucci, J. Tomasi, *J. Chem. Phys.* **1997**, *107*, 3032; b) B. Mennucci, E. Cancès, J. Tomasi, *J. Phys. Chem. B* **1997**, *101*, 10506; c) B. Mennucci, J. Tomasi, *J. Chem. Phys.* **1997**, *106*, 5151; d) M. Cossi, G. Scalmani, N. Rega, V. Barone, *J. Chem. Phys.* **2002**, *117*, 43.

Received: June 10, 2008
Revised: July 30, 2008